J. Phys. D: Appl. Phys. 26 (1993) 1333–1350. Printed in the UK

REVIEW ARTICLE

Time-reversal mirrors

Mathias Fink

Laboratoire Ondes et Acoustique, ESPCI, Université de Paris VII,
URA CNRS 1503, 10 rue Vauquelin, 75231 Paris cedex 05, France

Received 26 March 1993

Abstract. Time-reversal of ultrasonic fields allows a very efficient approach to focus pulsed ultrasonic waves through inhomogeneous media. Time-reversal mirrors (TRMS) are made of large transducer arrays, allowing the incident acoustic field to be sampled, time-reversed and re-emitted. This paper introduces the time-reversal approach in a discussion of the techniques used in optics for focusing through inhomogeneous media. The discussion is extended to ultrasonic pulsed fields where adaptative time delay focusing and TRM focusing are the main techniques of interest. Time reversal focusing of a pulsed wave is shown to be optimal in comparison with time delay focusing in the sense that it realizes the spatiotemporally matched filter to the inhomogeneous propagation transfer function between the array and the target. Time-reversal processing also permits choice of any temporal window to be time-reversed, allowing operation in an iterative mode. In multi-target media, such a process converges on the most reflective target. In the case of an extended target, automatic resonances can be achieved. Applications of TRM are numerous and include medical applications (imaging, lithotripsy and hyperthermia) as well as non-destructive testing (NDT) and underwater acoustics. Experimental results obtained with 64 and 128 channel TRMS demonstrate the efficiency of this technique.

Introduction du Professeur P G de Gennes

Le renversement du temps est une obsession ancienne des physiciens; avec la mécanique quantique, c'est devenu une opération précise sur les fonctions d'onde, reliée de façon profonde à la parité et à la conjugaison de charge. Qui aurait pensé, il y a quelques années, que cette même opération aurait des effets intéressants en acoustique, avec des 'particules' neutres aussi banales que les phonons? C'est le mérite de Mathias Fink et de son équipe d'avoir inventé et construit ces miroirs à renversement du temps qui (i) son très accessibles à nos moyens électroniques et (ii) ont des applications étonnantes. Ce travail combine à merveille les aspects fondamentaux et appliqués, dans l'esprit que nous essayons de maintenir à l'Ecole de Physique et Chimie: l'esprit de Pierre Curie, lui-même un grand pionnier du rôle de la symétrie dans les lois physiques.

1. Introduction

Time-reversal invariance is a very rich and powerful concept in classical and quantum mechanics. It has an impact on all facets of physics and important applications in quantum field theory and particle physics. However, simple experimental evidence of this concept is difficult to obtain in the field of classical mechanics. To test the time reversal invariance of the motion of a complex system of particles requires introducing a 'mirror' of the time variable. In an 'image world' such a mirror exists by taking a motion picture of this system with high enough resolution, and after a given instant T, by running the film backwards we observe the time-reversed motion. In the 'real world' the reversal of motion can be ascribed to the change in initial conditions (positions and velocities) of the complex system. This requires preparation of a new initial distribution for the positions and velocities of each particle as the exact distribution at instant T with all velocities of each particle reversed. Such an experiment is usually difficult to carry out on macroscopic systems because of the large number of microscopic parameters involved. Thus an apparent irreversibility is observed.

0022-3727/93/091333+18$07.50

If experiments of this kind are to be considered only as 'thought experiments' in the field of mechanics, in the field of classical waves, where time reversal invariance also occurs, it may be achieved much more simply. It is in the field of ultrasonic wave propagation that time-reversal mirrors (TRMs) can be realized most easily with large ultrasonic piezoelectric transducer arrays. If time-reversal mirrors are of great interest as a tool in fundamental physics, their applications in problems using large ultrasonic transducer arrays are numerous, including medical applications (imaging, lithotripsy and hyperthermia) as well as non-destructive testing and underwater acoustics. In these applications, that require very narrow beam, high focusing performances are needed. However, large arrays may suffer from strong geometrical distortions which should be corrected. Besides, the focusing of ultrasonic waves becomes a difficult operation as soon as the medium of propagation contains heterogeneities (spatial variations of the compressibility and/or the density in biological tissues and in sea water, liquid–solid interfaces in non-destructive testing). In such conditions, the acoustic beam can be distorted and redirected, so that optimal focusing cannot be achieved. Compensation for these two kinds of distortion must be self-adaptive because the designer has no *a priori* knowledge of them. The use of a time-reversal mirror represents an original solution to this problem [1,2].

In the time-reversal process, we take advantage of the properties of piezoelectric transducers, namely their transmit and receive capabilities, their linearity and the capability of instantaneous measurement of the temporal pressure waveforms. The pressure field $p(\boldsymbol{r}_i, t)$ detected with a set of transducer elements located at positions $\boldsymbol{r}_i$ is digitized and stored during a time interval T. The pressure field is then resynthesized by the same transducers in a reversed temporal chronology (last in, first out). This is equivalent to the transmission of $p(\boldsymbol{r}_i, T - t)$. A time-reversal mirror consists of a one- or two-dimensional transducer array. Each transducer is connected to its own electronic circuitry that consists of a receiving amplifier, an A/D converter, a storage memory and most importantly a programmable transmitter able to synthesize a time-reversed version of the stored signal.

Such a time-reversal mirror allows one to convert a divergent wave issued from an acoustic source into a convergent wave focusing on the source. Unlike an ordinary mirror that produces the virtual image of an acoustic object, the TRM produces a real acoustic image of the initial source. The time-reversal process appears to be a new way to solve inverse problems in ultrasonic wave scattering. This process can be used to focus on a reflective target that behaves as an acoustic source after being sonified. The method works even if there is an inhomogeneous medium between the target and the mirror.

The TRM is a generalization of an optical phase conjugated mirror (PCM) in the sense that it applies to pulsed broadband signals rather than to monochromatic ones. A comparison of these concepts shows that, in contrast to PCM, that works in continuous mode, TRM processing permits choice of any temporal window to be time-reversed. This allows operation in an iterative mode. In multi-target media, this process converges on the most reflective target. In the case of an extended target, automatic resonances can be achieved.

This paper introduces the time-reversal approach through a discussion of the two different techniques used for focusing in inhomogeneous media in optics, namely active optics and phase-conjugated mirrors. The discussion will be extended to ultrasonic pulsed fields where adaptive time-delay focusing techniques and TRM focusing processing are the analogous techniques. In contrast to adaptive time-delay focusing techniques, which can only correct distortions produced by a thin aberrator located close to the transducer array, TRM focusing is shown to compensate for distortion wherever the aberrator is positioned.

It is shown that TRM focusing is optimal in the sense that it realizes the spatiotemporally matched filter to the propagation transfer function through inhomogeneous media. It is a self-adaptive technique that compensates for any geometrical distortions of the array structure as well as for distortions due to propagation through inhomogeneous media.

This research was aimed initially at overcoming lithotripsy (biological stone destruction) limitations. In state-of-the-art lithotripsy, the determination of stone position is achieved with either an ultrasonic scanner or an x-ray imaging unit. Although the stone position may be accurately determined with x-ray systems, focusing of the destructive ultrasonic wave through inhomogeneous tissue remains difficult. Sound speed inhomogeneities can distort and redirect the ultrasonic beam. An even more crucial problem is related to stone motion due to breathing. The movement amplitude can be as large as 2 cm and stone tracking is needed for efficient therapy. The time-reversal process can solve these problems. The goal is to locate a given reflecting target among others, as for example, a stone in its surroundings (other stones and organ walls). The region of interest is sonified by the transducer array. The reflected field is sensed on the whole array, time-reversed and retransmitted. As this process is iterated, the ultrasonic beam will select the target with the highest reflectivity. If the target is spatially extended, the process will converge on one spot, whose dimension depends only on the TRM geometry and the wavelength. High amplification of the last iteration can be used in stone destruction.

Another application of TRM techniques has been developed in our laboratory in the field of non-destructive testing of metallurgical samples. Current ultrasonic inspection techniques require that the sample be immersed in a water tank. Very small metallurgical defects have to be detected through liquid–solid interfaces of any geometrical shape and the incident beam can be strongly distorted by the geometry of these liquid–solid interfaces. Focused transducers with special lens design have been built to overcome these limitations. Such transducers have a focusing lens

designed to make all the propagation times between the transducer surface and the focal point equal, thus providing optimum focusing at this point. However, these transducers are designed to focus ideally on only one point of the solid. Unfortunately, industrial inspections on thick samples require many different transducers and are quite expensive and time-consuming. The use of a time-reversal mirror (TRM) represents an original solution to this problem. It realizes in real time a focusing process matched to the defect shape and to the propagation medium.

Experimental results and various applications are described for 64 and 128 channel time-reversal mirrors and demonstrate the possibility of robust focusing through an inhomogeneous medium, as well as the efficiency of the iterative mode for focusing on the most reflective target.

2. Optical focusing in inhomogeneous media

Let us recall the two existing solutions for focusing in inhomogeneous media.

2.1. Active optics

Active optics techniques utilize deformable mirrors or mirror arrays whose profiles are adapted to distortions of the optical waveform coming from the source. In astronomy the source is active, as for example a bright star which is observed through the atmospheric turbulence. In other cases the source can be passive, as for example a target reflecting an illuminating wave. In most cases, profile optimization is performed by maximization of some function of the incoming radiation sensed by the mirrors [3, 4]. We note that active optics is a receive-mode technique requiring one-way propagation through the inhomogeneous medium.

2.2. Phase-conjugated mirrors

In contrast to classical mirrors that reflect an incident wavefield and produce a virtual image of the optical object, a PCM reflects and conjugates the incident wavefield to produce a real image of the object on itself. A major application of this technique is compensation of distorted wavefronts [5]. The distortion of the incident field induced by propagation through the inhomogeneous medium is exactly compensated when the conjugated wave propagates back towards the source. Therefore the technique requires two-way propagation in order to achieve focusing of the wavefront on the source. This technique works in the monochromatic mode and takes advantage of nonlinear properties of photorefractive crystals or of stimulated Brillouin effects in gases.

These two families of techniques can be extended to any kind of radiation field.

3. Ultrasonic focusing in inhomogeneous media

In the ultrasonic domain, two peculiarities allow a new approach to the focusing problem. The mean sound speed is low relative to the speed of light (1.5×10^3 m s^{-1} versus 3×10^8 m s^{-1}). This permits, with standard electronics, measurement of the time of flight between the source and the transducers. Moreover, piezoelectric transducers are linear devices with a very short impulse response that deliver an instantaneous signal proportional to the acoustic pressure. While optical sensors are sensitive to the average light intensity over their response time, which is always many times longer than the light period, in acoustics, all details of the temporal modulation of the pressure field can be recorded as long as we employ an adequately sampled transducer array with a sufficiently brief impulse response. In optics, the only way to acquire richer local information than the intensity is to use coherent illumination and record its interferences with a reference beam. This is currently performed in holography in which the interference pattern is uniquely related to the local phase of the wave. However, this information is considerably poorer than that contained in the temporal modulation of the pressure field which corresponds, for broadband pulsed fields, to knowledge of the amplitude and phase of all spectral components.

With these piezoelectric transducer properties, new working modes can be considered that generalize, for pulsed acoustic signals, optical techniques developed for continuous waves.

3.1. Adaptative time-delay focusing techniques

Adaptative time-delay focusing techniques are based, not on the use of mirrors whose profiles can be adapted, but on the use of transducer arrays. If a point source or point target is available in the region of interest, the most general approach consists of evaluation of a compensating time-delay characteristic which is superposed on the spherical one [6, 7]. The echoes from the target drive the array. The received signals are cross correlated and the proper time delays are determined by the time shift corresponding to the maximum of the cross correlation between signals from neighbouring transducer elements. Although cross correlation techniques are very attractive, they suffer from two important limitations. One is related to the nature of target available in the medium. The other limitation results from the nature and location of the inhomogeneous medium.

The first limitation of the cross correlation technique is that a beacon signal cannot be expected everywhere in the medium. Different authors have shown that a point-like target can be replaced by a random distribution of scatterers like those in biological tissues [6–10]. The cross correlation technique is then applicable because of the spatially incoherent nature of the backscattered field. Spatially incoherent sources are obtained if the

size of and mean distance between individual scatterers are typically much smaller than the resolution cell of the focusing array. In this case, neighbouring transducers will sense echographic signals that are highly correlated [11]. However, when the region of interest contains one or several specular reflectors of extended dimension, the cross correlation technique is not applicable because of the spatially coherent nature of the reflected field. A kidney stone or a bone have a size greater than the wavelength and the individual echoes originating from these reflectors can be very different from one transducer to the other and then difficult to cross correlate. In NDT, extended defects with low contrast are difficult to detect, as for example the so-called hard α defects in titanium samples. In the case of a medium containing several reflectors, the echo pattern becomes so complicated that the cross correlation technique cannot converge.

Another limitation of the cross correlation technique comes from the fact that this method reduces to the determination of a time delay across the array. Time-delay focusing is a valid technique in homogeneous media. It can also correct for unknown geometrical distortion of the array and for the effect of a thin aberrating layer located close to the array. Indeed, thin random layers as well as time-shift errors due to any geometrical distortion act only as random time delays, variable from one transducer element to another. In optical astronomy, this hypothesis is valid as long as the atmospheric turbulence is confined close to the telescope and far from the stars. In most medical applications this hypothesis is false: we always work in the near field of the transducers and the inhomogeneities are distributed over the whole volume. A wave propagating in such an inhomogeneous medium is not only delayed, but its spatial and temporal shape is also distorted through refraction, diffraction and multi-scattering. The adaptive delay-line focusing technique no longer works when the array probe–aberrator distance increases [12]. In such cases optimal focusing cannot be achieved with only delay-line techniques. Optimal focusing, valid for any kind of inhomogeneous medium, needs to take into account all the information received on the array from the point source (such as time delay and waveform modifications of the individual signals recorded on each transducer element).

3.2. Time-reversal of ultrasonic fields: basic principles

Time-reversal processes represent an original solution to these different problems. Time-reversal processing takes advantage of the invariance of the wave equation under a time-reversal operation [1, 2]. This means that if we want to focus in the transmit mode through any inhomogeneous medium or through a liquid–solid interface, it is adequate to record the distorted wavefield coming from a source (active or passive) located at the desired focal point and to time-reverse this field. The time-reversed wavefield back-propagates through the inhomogeneities and optimally refocuses on the source [1, 2].

Time-reversal invariance of the wave equation is valid only in the frequency range where the medium can be assimilated to a lossless propagating medium. In a fluid medium with compressibility $\kappa(\boldsymbol{r})$ and density $\rho(\boldsymbol{r})$ that vary with space, the acoustic pressure field wave equations reads [13]

$$\kappa(\boldsymbol{r})\frac{\partial^2 p}{\partial t^2} = \nabla\left(\frac{\nabla p}{\rho(\boldsymbol{r})}\right). \qquad (1)$$

Looking at this propagation equation, we note that it has a special behaviour with respect to the temporal variable t; indeed, it contains only a second-order time-derivative operator. This property is the starting point of the time-reversal principle, valid only for a lossless propagation medium. As an immediate consequence, if $p(\boldsymbol{r}, t)$ is a pressure field solution of the propagation equation, then $p(\boldsymbol{r}, -t)$ is another solution of the problem. This property is specific to the invariance under a time-reversal operation. In the case of an isotropic solid sample immersed in the fluid, the acoustic field is described in the solid by the acoustic displacement field $\boldsymbol{u}(\boldsymbol{r}, t)$ according to another time-reversal invariant wave equation [13]:

$$\rho_s\frac{\partial^2 \boldsymbol{u}}{\partial t^2} = (\lambda + 2\mu)\nabla(\nabla \boldsymbol{u}) - \mu\nabla \wedge \nabla \boldsymbol{u} \wedge \boldsymbol{u} \qquad (2)$$

where λ and μ are the Lame coefficients and ρ_s is the solid density. Strain and stress continuities allow us, from the knowledge of $\boldsymbol{u}(\boldsymbol{r}, t)$ in the solid, to determine a unique solution $p(\boldsymbol{r}, t)$ for the pressure field in the liquid. As an immediate consequence of the time-reversal invariance of equation (2), if $\boldsymbol{u}(\boldsymbol{r}, t)$ is the displacement field in the solid, then $\boldsymbol{u}(\boldsymbol{r}, -t)$ is another solution of the problem and is related through the strain and stress continuities to the time-reversed pressure solution $p(\boldsymbol{r}, -t)$ in the fluid.

These properties of time-reversal have been observed by Stokes [14] in the framework of the classical experiment of reflection and transmission of a plane wave along the interface separating two media of different sound velocity. Considering a plane incident wave of amplitude 1 propagating from medium 1 to medium 2, we can observe a reflected plane wave of amplitude R and a transmitted wave of amplitude T (figure 1(a)). Starting from this configuration in which the pressure field $p(\boldsymbol{r}, t)$ results from these three plane waves, Stokes tried to find out whether or not this experiment could be time-reversed. He used the plane wave property that time-reversal can be accomplished by reversing the wavevector direction. Thus, the time-reversed solution $p(\boldsymbol{r}, -t)$ can be described by a new set of three waves: two incident waves of amplitude R incident from 1 to 2 and of amplitude T incident from 2 to 1, followed by a transmitted wave of amplitude 1 propagating in medium 1 (see figure 1(b)). It can easily be verified that this new solution $p(\boldsymbol{r}, -t)$ is also a solution of the wave equation. Indeed, defining R' and T' as the reflection and transmission coefficients for an incident wave coming from medium

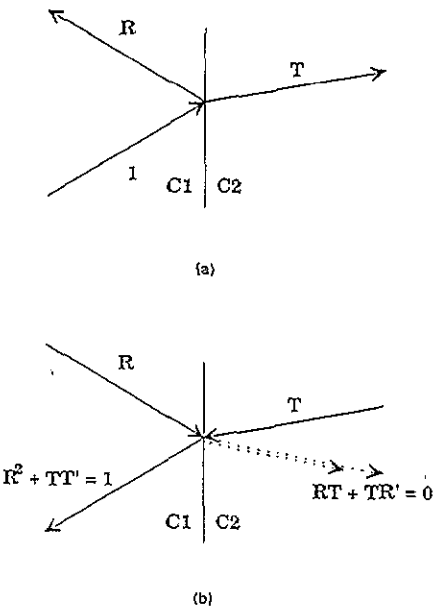

Figure 1. (*a*) Reflection and transmission of a plane wave along the interface separating two media of different sound velocities. (*b*) Time-reversal of (*a*).

2, we see from the superposition principle that the two incident waves lead to generation of four plane waves, two of them propagating in medium 1 with a resulting amplitude $R^2 + TT'$, and the other two propagating in medium 2 with a resulting amplitude $RT + TR'$. An elementary computation of the reflection and transmission coefficients R, T, R' and T' allows us to verify the following relations:

$$R^2 + TT' = 1 \qquad (3a)$$

$$R + R' = 0. \qquad (3b)$$

Thus this example shows that the wave equation can be directly interpreted as the time-reversal of the previous situation.

In fact, these arguments can be generalized for different kinds of incident acoustic fields and other geometries of inhomogeneities. It is important to note that the two relations written above are only valid if the reflected and transmitted plane waves have a real wavenumber (propagative). In a more general situation, the incident field contains evanescent components. Evanescent waves can be created at interfaces by incidence at specific angles or, for example, when an incident ultrasonic beam is scattered by a medium whose compressibility $\kappa(\boldsymbol{r})$ contains spatial-frequency components of linear dimensions that are, roughly speaking, smaller than the wavelength. Evanescent waves cannot be time-reversed since their directions of propagation are undefined [15]. Superposition of propagative and evanescent waves leads to limitation of the time-reversal process, and the basic theory must be analysed carefully. Owing to the finite bandwidth of the incident field, some information is lost in the time-reversal process.

3.2.1. The time-reversal cavity. In any propagation experiment, initial conditions (acoustic sources and boundary conditions) determine a unique solution $p(\boldsymbol{r}, t)$ in the fluid. Our goal, in time-reversal experiments, is to modify the initial conditions in order to generate the dual solution $p(\boldsymbol{r}, -t)$. However, due to causality requirements, $p(\boldsymbol{r}, -t)$ is not an experimentally valid solution. Therefore, we will limit ourselves to generation of $p(\boldsymbol{r}, T - t)$.

One solution to the difficult problem of generating the time-reversed solution consists in measuring during a time interval T the pressure $p(\boldsymbol{r}, t)$ in the whole three-dimensional volume (T is long enough that the pressure field vanishes for $t > T$), and then retransmitting throughout the volume $p(\boldsymbol{r}, T - t)$. This solution is unrealistic since it requires sampling the whole volume with transmit–receive probes. A more realistic solution takes advantage of the Huygens principle: the wavefield in any point of a volume can be predicted from knowledge of the field and its normal derivative on a closed surface surrounding the volume. Therefore, the time-reversal operation is reduced from a three-dimensional volume to a two-dimensional surface. Indeed, knowledge of the pressure field and its normal derivative at any point of a closed surface is sufficient to predict the pressure field inside this surface [16].

Starting from this point of view, focusing on a target in an inhomogeneous fluid medium can be treated in the following way. A point-like source located in an inhomogeneous medium creates a spherical wavefront that is distorted after propagation in the medium. We consider a closed surface surrounding the object source and the inhomgeneities, and we assume that we are able to measure the pressure field and its normal derivative at any point on the closed surface (figure 2(*a*)). In a second step, we assume that we are able to create secondary sources (monopole and dipole sources) on the surface that correspond to time-reversal of the signals measured during the first step. As a result of the secondary sources created on the surface, a time-reversed pressure field back-propagates inside the surface and is distorted by interaction with the inhomgeneities.

Under such conditions, it can be shown [17, 18] that the time-reversed pressure field is focused on the initial source position (figure 2(*b*)). It is important to note that the time-reversal technique provides better focusing than the correlation technique: in particular, it is not necessary to assume that the inhomogeneities are only located in the neighbourhood of the transducer array, and to assume that the effects of inhomogeneities reduce to a simple time delay varying from one transducer element to another.

The efficiency of time-reversal techniques obtained from closed cavities has been analysed for weakly and strongly inhomogeneous media [18], and it is shown that the time-reversed pressure field is focused on the initial source position. However, the finite spectral bandwidth of ultrasonic signals restricts resolution because the spatial scales of inhomogeneities that are smaller than the minimum wavelength are blurred. Therefore, generation of $p(\boldsymbol{r}, T - t)$ in the whole volume is not perfect [18].

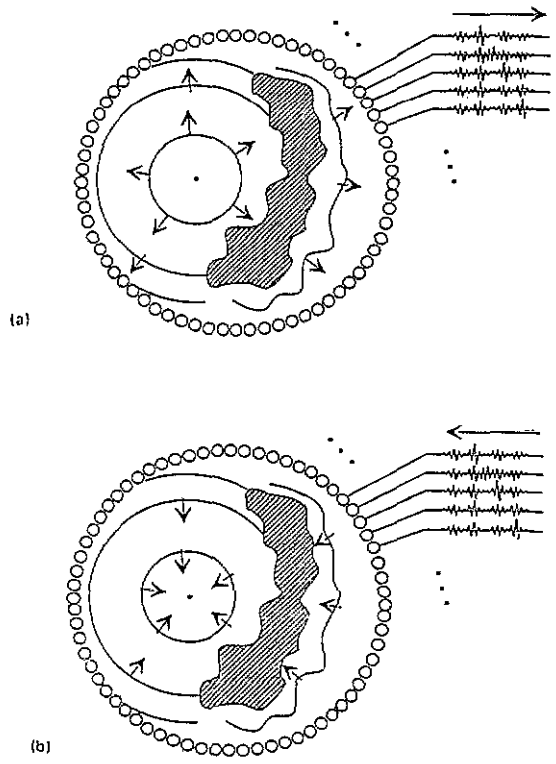

Figure 2. Time-reversal cavity. (*a*) Recording step. A closed cavity is filled with transducer elements. A point-like source generates a wavefront which is distorted by heterogeneities. The distorted pressure field is recorded on the cavity elements. (*b*) Time-reversed or reconstruction step. The recorded signals are time-reversed and re-emitted by the cavity elements. The time-reversed pressure field back-propagates and refocuses exactly on the initial source.

3.3. The time-reversal mirror

The time-reversal cavity is, of course, an ideal concept for focusing through inhomogeneous media. Unfortunately, such a cavity is difficult to realize in practice. The strongest limitation is linked to the difficulty of surrounding the focal region by a set of transducers. In medical applications, as well as in non-destructive testing, we usually work in pulse-echo mode and the probe is located only on one side of the region of interest. This mode of operation is more practical and allows focusing from an array of transducers. In this case, the time-reversal cavity may be replaced by a time-reversal mirror. Such a mirror can be plane or prefocused, one-dimensional or two-dimensional. However, its ability to focus through aberrating media may be comparable to that of a closed cavity.

Other limitations of TRM, even in homogeneous media, are the same as those observed in classical focusing with delay-line techniques.

(i) Diffraction effects act as a low-pass filter on the spatial frequency spectrum of any wavefield. The resulting image of a point is a spot with dimension that depends on the wavelength.

(ii) The limited dimension of the TRM induces a point spread function whose width is related, as in classical focusing techniques, to the angular aperture of the mirror observed from the focal point.

(iii) Spatial sampling of the TRM by a set of transducers introduces grating lobes. These lobes can be avoided by using an array pitch of the order of $\lambda/2$, where λ is the central wavelength of the pressure field. However, such a fine sampling is not necessary if the TRM is prefocused on the region of interest (cylindrical or spherical mirror).

(iv) Temporal sampling of the data recorded and transmitted by the TRM has to be comparable to that of the time-delay law in classical time-delay focusing. A maximum rate of $T/8$ (T is the central period) is needed to avoid secondary lobes [19].

3.3.1. Echographic focusing with a TRM. As illustrated in figure 3, time-reversal focusing on a target through inhomogeneous media requires three steps. The first step consists of transmitting a wavefront through the inhomogeneous medium from the array to the target. The target generates a scattered pressure field that propagates through the inhomogeneous medium and is distorted. The second step is a recording step: the backscattered pressure field is recorded by the transducer array. In the last step, the transducer array synthesizes the time-reversed field. This pressure field propagates through the aberrating medium and focuses on the target. In the case of a weak inhomogeneous medium that satisfies the first Born approximation (a single scattering process), the TRM is able to compensate exactly for the wavefront distortion whatever the aberrator position in the ultrasonic beam [20–23]. This is demonstrated by the experimental results presented in [24].

However, a limitation of the TRM compared with the closed cavity appears in the case of very strong inhomogeneities. In such a case, multiple scattering processes limit TRM efficiency. First, it is necessary to measure the pressure field on a very long time interval to take into account the multiple scattered waves that decay slowly. Second, the scattered field is radiated in all directions and a mirror cannot measure the complete information needed to optimize the true reversal. In comparison, in a weakly inhomogeneous medium that induces only single scattering, measurement of the distorted pressure field requires a shorter time. Moreover, time reversal of the field recorded on only one plane is sufficient to achieve optimal focusing on the target.

3.3.2. The TRM experimental arrangement. Experimental data on time-reversal mirrors have been obtained by Wu and Thomas with different real-time electronic prototypes made of 64 or 128 channels working in transmit–receive mode [24]. The transmission module is made of 128 programmable transmitters. Each programmable transmitter is driven by a 32 Kbyte buffer memory through a 12-bit D/A converter operating at 40 MHz sampling rate. Each converter is followed by a linear power amplifier. The transmitter delivers 30 V peak-to-peak voltage to a 50 Ω transducer impedance.

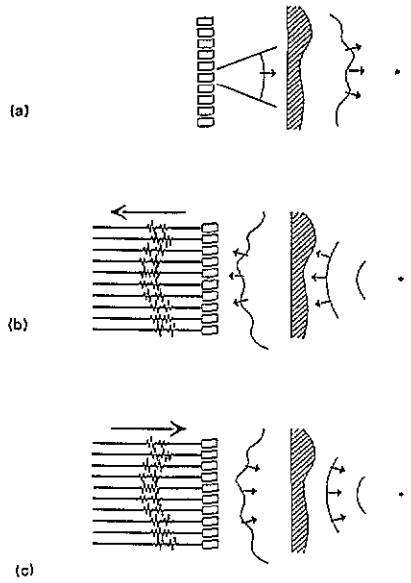

Figure 3. The TRM focusing through inhomogeneous media requires three steps. The first step (*a*) consists in transmitting a wavefront through the inhomogeneous medium from the array to the target. The target generates a backscattered pressure field that propagates through the inhomogeneous medium and is distorted. The second step is the recording step (*b*); the backscattered pressure field is recorded by the transducer array. In the last step (*c*) the transducer array generates on its surface the time-reversed field. This pressure field propagates through the aberrating medium and focuses on the target.

In the transmit mode the 128 transmitters work simultaneously and are connected to 128 elements of one- or two-dimensional transducer arrays.

Two steps are required in the receive mode: amplification and A/D conversion. We use a set of 16 A/D converters through a multiplexer, so that recording a complete set of A lines requires eight consecutive emissions. A set of 16 logarithmic amplifiers allows the recording of a 90 dB instantaneous dynamic range through the 16 A/D converters. Recorded data are digitized at a sampling rate of 40 MHz with a 10-bit dynamic range. Exponentiation of the data is made in each buffer memory to correct the logarithmic operation before the time-reversal operation. A Compaq 486 computer controls the time-reversal process and the matching of the dynamic range between receive and transmit modes. The prototype allows a complete 128 channel time-reversal operation in less than 10 ms and different one- and two-dimensional arrays have been designed for these experiments.

3.4. Experimental results

3.4.1. Focusing compensation for a geometrically distorted array. The first experiment was conducted with a prefocused one-dimensional cylindrical time-reversal mirror (TRM1) made of a linear array of 64 elements working at 3.5 MHz ($\lambda = 1.5$ mm). Each of the transducer elements is rectangular, 0.5 mm wide and 10 mm high. The array pitch is 0.6 mm and the elements are set out on a cylindrical backing of 80 mm radius of

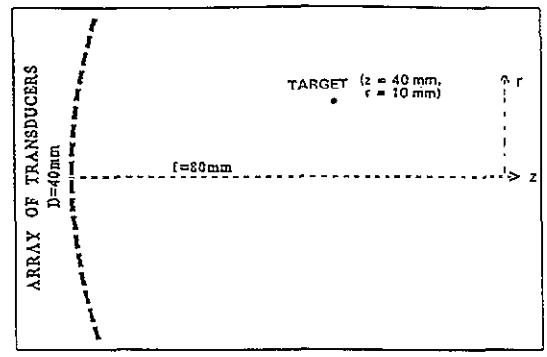

Figure 4. Configuration of the off-axis self-focusing experiment with TRM1. The cylindrical mirror aperture is 40 mm long and the focal length is 80 mm. The target is a needle-point hydrophone located at $z = 40$ mm from the array surface and at 10 mm off axis.

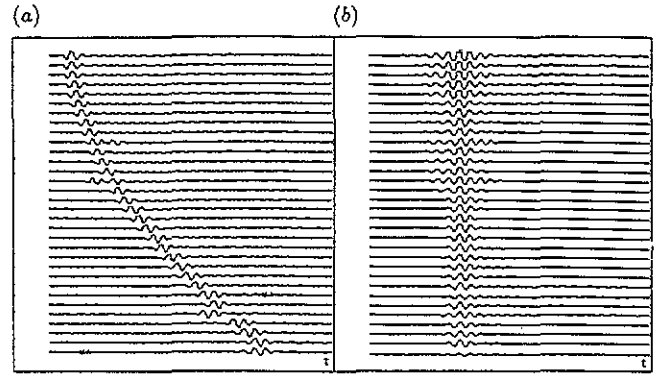

Figure 5. (*a*) Individual pressure signals recorded by each TRM1 element when the hydrophone is used as the transmitter. Note that two transducers are out of line. (*b*) Individual pressure signals recorded by the hydrophone corresponding to the individual transmission of the time-reversed signals of (*a*). Note that all the time-reversed waves reach their maximum at the same time.

curvature (figure 4). The total aperture of TRM1 is thus equal to 40 mm with an 80 mm natural focal length. This array suffers from geometrical distortions. Two elements are out of line and record pulse-echo signals shifted by more than 0.8 μs relative to the adjacent elements. The experiment is performed using a needle-point hydrophone as an active transmitting point source. The cylindrical array and the point source are immersed in a water tank. The hydrophone location r_0 is far from the geometrical focus of TRM1. It is located at a depth $z_0 = 40$ mm from the surface of the mirror and 10 mm away from the array axis corresponding to the coordinates $r_0 = (40$ mm, 10 mm), see figure 4.

The pressure wave transmitted by the hydrophone is recorded on the 64 elements of TRM1. Of the corresponding signals, 32 are shown in figure 5(*a*). They line up according to an oblique cylindrical law corresponding to the location of the out-of-focus source. We observe that two transducers of the array are out of line. They deliver pressure signals before the neighbouring transducers.

The time-reversal experiment was conducted in two steps. In the first, the individual signal recorded by each transducer is time-reversed and transmitted alone. The

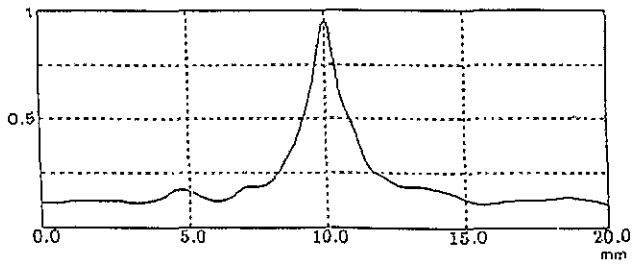

Figure 6. Directivity pattern (maximum of pressure field) in the plane $z = 40$ mm. All the TRM1 transducers transmit simultaneously the time-reversed signals of figure 5(*a*).

hydrophone is now used in the receive mode to control the pressure field at the initial location of the source. Figure 5(*b*) shows individual signals measured by the hydrophone corresponding to the individual transmission of each transducer element of TRM1. All the individual time-reversed waves reach their maximum at the same time T at the source location r_0 as predicted by the TRM matched-filter performance. In the time-reversal process earlier signals corresponding to the shorter transit times are retransmitted later, such that all the individual signals reach their maximum at the same time. The time-reversal process cancels the defects of the array.

In the second step, all the elements simultaneously retransmit the time-reversed field of figure 5(*a*), therefore resulting in constructive interference of all the individual waves of figure 5(*b*) at time T at the source location r_0. The TRM focusing pattern is obtained by scanning the plane $z = 40$ mm with the hydrophone working in the receive mode. The maximum of the pressure field is computed for each hydrophone position. Figure 6 represents the directivity pattern. It reaches a maximum at the initial source position r_0 (40 mm, 10 mm). This experiment shows that TRM focusing is self-adaptive and accomplishes automatic compensation for geometrical distortions of the array.

3.4.2. Focusing through a random aberrating layer. In this set of experiments, we used a one-dimensional plane time-reversal mirror (TRM2) made of a plane linear array. The array pitch is 0.75 mm and the working frequency is 3.5 MHz. The target is observed through a strongly aberrating medium. The experiment is carried out for different TRM–aberrator distances. The aberrating medium is made of a rubber layer in which the thickness is randomly modulated. The ultrasonic velocity in the rubber is about 1200 m s^{-1}. The layer is shaped with a random profile in the lateral direction and a uniform thickness in elevation. The random profile induces a random shift on the layer transit time, whose standard deviation is about 0.15 μs compared with the acoustic period 0.3 μs of TRM2. The set of experiments was done in two steps. The first step investigates the distortions introduced by the layer on cylindrical beam-forming experiments. Cylindrical beam-forming delays are computed in order to focus through homogeneous water at 90 mm from the surface of the array and along the array centre line. The 64 elements transmit an identical pulse through the calculated bank of delay lines and a needle-point hydrophone scans the focal plane ($z = 90$ mm) for different positions of the aberrating layer. Figure 7 shows the directivity pattern measured in the focal plane (maximum of the pressure field at $z = 90$ mm) when the aberrator is located at different depths from the linear array. These figures correspond to an array–aberrator distance d of respectively 0, 27, 47 and 67 mm. The appearance of these figures clearly shows that the maximum defocusing effect is observed for $d = 0$ mm, which corresponds to the aberrator being against the array. The beam is widely spread. The −6 dB lateral resolution is about 6 mm and the side-lobe level is very high. The −6 dB lateral resolution corresponds to the focusing of an apparent transmitting aperture smaller than the 48 mm long TRM2 aperture. Figure 7 shows that beam spreading is reduced when the probe–aberrator distance increases, since the focused beam intercepts a smaller area of the aberrator. The second step of the experiment illustrates the time-reversal focusing process. The hydrophone is used as a point-like reflector located at a depth $z = 90$ mm. For each TRM–aberrator distance, the point reflector is illuminated through the aberrating layer by incident beams corresponding to the pressure fields of figure 7. The echoes from the hydrophone are distorted by the rubber layer and are recorded on the array (see for example figure 8(*a*) for $d = 0$ mm and figure 8(*b*) for $d = 27$ mm). The corresponding signals are time-reversed and re-emitted. The time-reversed waves propagate through the aberrator and the time-reversed pressure field is measured by scanning the focal plane with the same hydrophone now working in the receive mode. Figure 9 shows the resulting focal beams for $d = 0$, 27, 47 and 67 mm. The four directivity patterns are similar and correspond to −6 dB lateral resolution of about 1.5 mm. These results demonstrate the efficiency of time-reversal focusing for compensating for distortions induced by aberrators whatever the probe–aberrator distance [8]. Figure 10 shows the results obtained with the adaptive time-delay focusing technique. The time-delay focusing law is obtained by the cross correlation technique from the data of figure 8. We can observe that, for large distances, adaptive time-delay focusing does not help.

In the last part of this section, we wish to discuss a very fundamental point about focusing processes through inhomogeneous media. Focusing with TRM seems to be a complicated technique because it requires transmission of a different waveform from each transducer element, while, in the time-delay technique, it reduces transmission of the same pulse within a time-delay from each element. Time-delay focusing is a valid technique only to correct for the effect of an aberrating layer located close to the array. Indeed, the thin random layer acts only as a random propagating delay. A spherical wave originating from a point source is then delayed by propagation through the aberrating layer. The individual pressure signals recorded along the output plane of the aberrator are only delayed. Their shapes are identical, only their arrival times are randomly modified. This is clearly shown in figure 8(*a*) which corresponds to

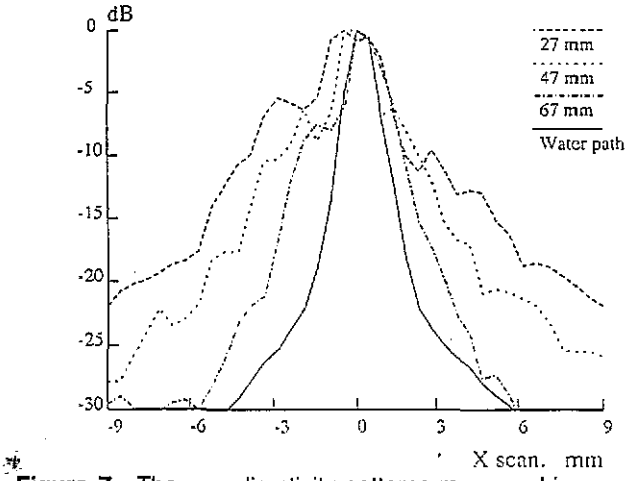

Figure 7. The TRM2 directivity patterns measured in the plane $z = 90$ mm. Here TRM2 is a plane transducer array and a random aberrating layer is located between the array and the scanned plane. This figure shows the *directivity patterns measured with a cylindrical beam-forming* technique corresponding to an array–aberrator distance d of respectively 0, 27, 47 and 67 mm.

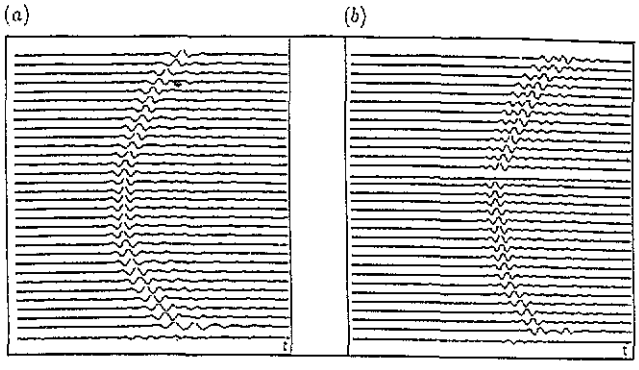

Figure 8. Echographic signals recorded on the array from the hydrophone for two different array–aberrator distances. $d = 0$ mm (*a*) and $d = 27$ mm (*b*).

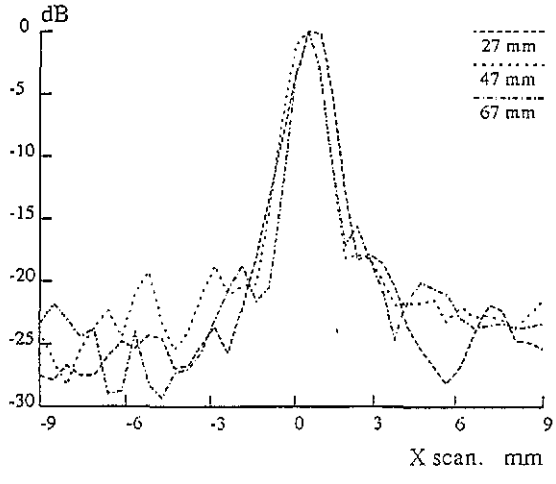

Figure 9. This shows the directivity patterns for the same array–aberrator distances as in figure 7 with the TRM focusing technique.

the hydrophone echoes propagating through the aberrator and recorded when the array–aberrator distance d =

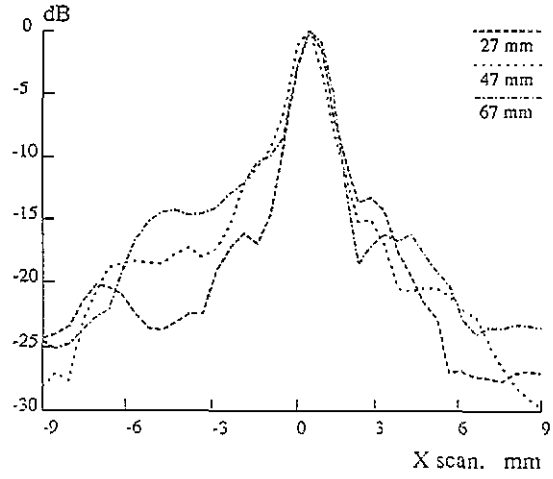

Figure 10. Directivity patterns for the same array–aberrator distances as in figure 7 with the adaptive time-delay focusing technique.

0 mm. In this case, transmitting the time-reversed version of figure 8(*a*) or transmitting an identical pulse through matched delay lines will give the same focusing results.

However, when the array–aberrator distance increases, the recorded pressure signals originating from a point source are not only delayed, but also their shapes are no longer similar. Figure 8(*b*) shows the signals recorded by TRM2 from the hydrophone when $d = 27$ mm. The strong distortions of the recorded signals and the complicated shape of this pattern result from propagation of the pressure field from the output plane of the layer towards the array recording plane ($d = 27$ mm). Although the pressure signals are identical within a time delay on the output layer plane, the interference between all the Huygens wavelets originating from this plane results in a complicated pattern which has lost shape invariance. In this case, time-reversal focusing is the only valid technique for refocusing [8]. Delay-line focusing techniques lose their efficiency when the probe–aberrator distance increases.

3.4.3. Auto-adaptive focusing in solid media: applications to NDT. These experiments were performed with a two-dimensional prefocused array working at 3 MHz (TRM3) by Chakroun [25]. TRM3 is a prefocused spherical mirror with a 200 mm radius of curvature made of 121 elements. The central element is a plane disc and the others are annular sector elements. The transducers are distributed according to a structure of six annuli of respectively 1, 8, 16, 24, 32 and 40 elements (figure 11). The total aperture is equal to 60 mm and the mirror is immersed in a water tank. The samples of interest were made of titanium. Titanium is a noisy medium in the sense that it gives rise to a strong ultrasonic speckle noise related to a heterogeneous microstructure. The block of titanium is located in front of the mirror. The working frequency of TRM3 is 3 MHz ($\lambda = 0.5$ mm in the water and $\lambda = 2$ mm for a longitudinal wave in the titanium sample). The experiments were performed to detect

a particular type of defect which can be observed in titanium: the hard α. The hard α is a small defect of irregular and unknown shape and of small acoustic impedance contrast. This defect has a backscattered amplitude field equivalent to a 0.4 mm diameter flat bottomed hole. It is located inside a block of titanium set at 20 mm depth and 5 mm off axis. In the first step, TRM3 illuminated a sector containing the hard α defect. The large illuminating beam was transmitted by a single transducer element located at the centre of the array. After the first illumination, the echoes from the block were recorded. Figure 12 (reception 1) presents the recorded data in grey level for each of the 121 transducer elements. The data are represented in B mode, where the horizontal axis represents the time arrival of the echo (depth) and the vertical axis the transducer numbers. The transducer number is 1 at the top of the figure and increases towards the bottom. From these data we see the two echoes coming from the interfaces between titanium and water. Between these echoes we can observe the titanium speckle noise. In the second step of the experiment we select for each of the recorded data a 2 μs time window after the front face echo. These windows are time-reversed and retransmitted. The time-reversed waves propagate and are refocused on the hard α and we recorded again the echoes coming from the block. Figure 13 (reception 2) presents the new recorded data. We always observe echoes from the two interfaces, but between these echoes an oscillating line appears. This line corresponds to echoes from the hard α received by the TRM elements. The amplitude of the oscillation corresponds to an off-axis defect, whose wavefront intercepts obliquely the two-dimensional array. We can add all these data for all the elements, and the corresponding sum is presented on the left-hand part of the figures. A 40 dB improvement of the signal to speckle-noise ratio is observed in this figure relative to the target level before the time-reversal process. The important point to be noticed here is the different behaviour of time-reversal on echographic speckle noise compared with hard α echo. In titanium the speckle noise originates from the very thin microstructure whose dimension is of the order of $\lambda/100$. A time-reversal process cannot time-reverse this kind of waveform due to the loss of information during propagation with a 3.5 MHz central frequency. However, the small coherent echographic signal originating from the defect can be time-reversed efficiently, and after one TRM process the level of this echo relative to the speckle-noise one has increased by nearly 40 dB. This kind of experiment can be conducted for different positions of the hard α defect in the illuminating field. The hard α defect is automatically detected in a section of more than 4 cm^2 around the mirror axis. These results demonstrate the ability of TRM to compensate for distortion induced by liquid–solid interfaces observed at oblique incidence, and to select a coherent echo from incoherent background noise.

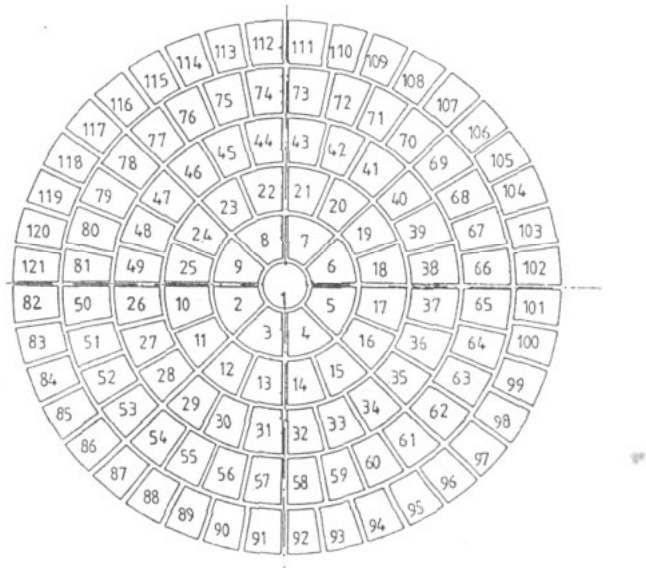

Figure 11. Geometry of the prefocused two-dimensional time-reversal mirror used in NDT.

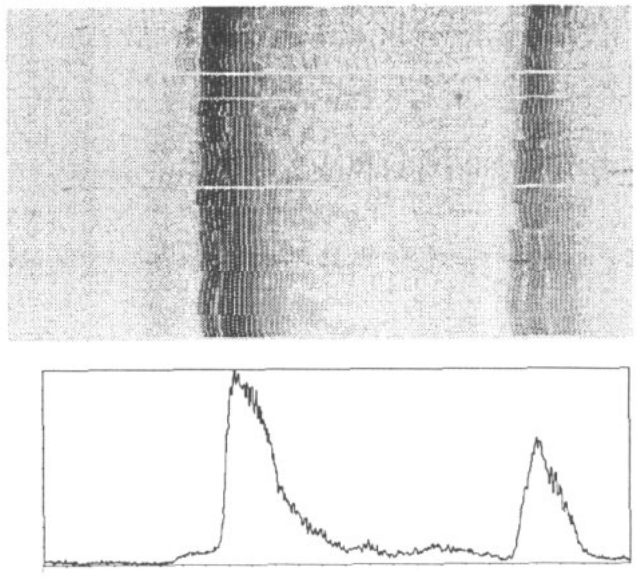

Figure 12. After the first illumination, the echoes from the titanium sample are recorded. The presentation is made in B mode. The horizontal axis represents the time (similar to depth in pulse echo mode) and the vertical axis the transducer number. Each individual echographic signal is then presented as a horizontal line modulated by the signal amplitude. The hard α defect was located 5 mm off axis of TRM3, and the echoes from the defect are not visible in the titanium noise. The lower part of the figure represents the summation of the recorded signals from all the transducer elements (logarithmic scale of 90 dB).

4. Comparison between time-reversal mirrors and phase-conjugated mirrors

The basic principle of a time-reversal mirror is an extension of an optical phase conjugated mirror. If $P(\boldsymbol{r}, \omega)$ is the temporal Fourier transform of $p(\boldsymbol{r}, t)$, then the temporal Fourier transform of $p(\boldsymbol{r}, -t)$ is $P^*(\boldsymbol{r}, \omega)$. Therefore, time-reversal of pulsed signals is equivalent to phase-conjugation of

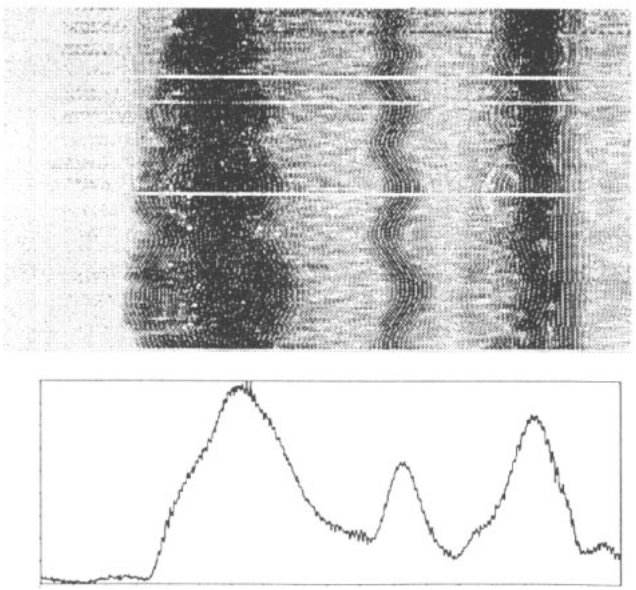

Figure 13. After one time-reversed transmission, the new reflected waves from the titanium are recorded. We can notice a wavefront appearing in the data which corresponds to the hard α defect. On the lower part of the figure, the summation of the data shows an improvement of the signal (from the hard α defect) to noise of 40 dB.

monochromatic waves. However, this equivalence is only valid mathematically and there are some fundamental differences between these two techniques.

4.1. Linearity versus nonlinearity

Since the time responses of optical detectors are very long relative to the period of optical waves, an optical phase-conjugated mirror (PCM) requires a nonlinear effect to measure and has to conjugate the phase information on monochromatic wavefields [5]. The optical phase conjugation can be understood as a real-time dynamic holographic method. Indeed, it is well known that the holographic technique allows generation of the complex conjugate of an incident monochromatic wave.

The basic principle of holography consists of superposition of the incident monochromatic wavefield on a reference wave and measurement of the resulting interference fringes on the holographic plate. The interference of two waves transforms the phase information of the incident wave, that is required to be known but not otherwise available, into intensity information that is experimentally available. This is a nonlinear process. After development of the holographic plate, a photographic transparency is obtained with the information on the incident wave and its complex conjugate. Appropriate illumination of this photographic transparency (for example the complex conjugate of the reference wave) leads to generation of the complex conjugate of the incident wave. This technique involves two reference waves, one during the recording step and a second one during the reading step (figure 14).

In the case of a PCM, the holographic plate is replaced for example by a nonlinear photorefractive

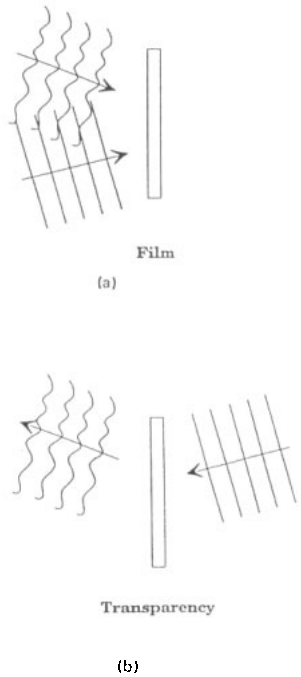

Figure 14. Principle of monochromatic phase-conjugated holography. The first step (*a*) consists in recording on the holographic plate of the interference fringes between the incident monochromatic wavefield and a reference plane wave. After development of the holographic plate, a photographic transparency is obtained. The illumination of this transparency (*b*) by the complex conjugate of the plane reference wave leads to generation of the complex conjugate of the incident wave.

medium ($LiNbO_3$, BSO,...) that spatially changes its photorefractive index (with a time response of a few tens of milliseconds) in reaction to the interference of the incident wave with one of the reference waves. The refractive index changes are due to electro-optic effects. Interference between the incident beam and the reference beam results in phase-volume gratings in the photorefractive media. The second reference wave is then diffracted by this resulting grating, thus generating the complex conjugate of the incident wave. Several similar configurations can be realized either with this kind of wave mixing (four-wave mixing) or with other nonlinear techniques using the stimulated Brillouin scattering effect [5]. In all these techniques a wave incident on the PCM produces a phase-conjugated wave in a nonlinear medium.

In the time-reversal technique, wave mixing is not required and nonlinear effects are not necessary. They are replaced by the use of linear reversible transducers linked to a read–write memory. All these steps are linear. Additionally, phase-conjugation occurs in the whole volume of the photorefractive medium, while time-reversal occurs only on a two-dimensional surface area.

4.2. Continuous versus transient regime

In optics, once the photorefractive medium has modified its photorefractive index, a continuous state is reached. This means that the concept of time disappears from

the process. All continuous monochromatic waves generated in the aberrating media (single or multi-scattering) and in the photorefractive medium will interfere. This requires the laser coherence length to be much longer than the dimensions of the optical circuit. However, due to causality requirements, there is a transient period during which the different waves generated cannot interfere. In time-reversal experiments, ultrasonic signals are brief and all processes occur in the transient regime.

In the continuous regime, interference between the incident wave and any subsequent multiply reflected waves between the PCM and the aberrator plays a very particular role. It can be shown that the resulting interference between all these waves allows exact compensation of the distortion due to the aberrating medium. This compensation is achieved for weakly inhomogeneous media (first Born approximation) as well as for strongly heterogeneous media containing discontinuities [26–28].

The following experiment illustrates the particular role of the continuous regime in the case of a medium containing discontinuities [27,28]. Recall that a PCM works in a continuous mode and phase-conjugates an incident wave, for example a plane wave of amplitude 1 propagating in medium 1 of sound velocity c_1 (figure 15(*a*)), and consider the effect of inserting a new medium 2 of sound velocity c_2 between the source of the incident wave and the PCM (see figure 15(*b*)). An initial reflected wave of amplitude R and a transmitted wave of amplitude T result. The transmitted wave T is then phase-conjugated by the PCM. This phase-conjugated wave is reflected and transmitted through the interface 2 to 1. A new reflected wave comes back to the PCM with a new incidence and is phase-conjugated. The process repeats itself periodically. The main point is that the set of waves generated in medium 1 from all the phase-conjugated waves produces a resulting plane wave of amplitude 1 in the reverse direction of the incident wave and complete destructive interference in the direction of the initial reflected wave. Such a result means that, for an observer located in medium 1, insertion of medium 2 between medium 1 and the PCM does not change anything. The observer sees only the phase-conjugated wave of amplitude 1 with a reverse wavevector. This important result is linked to the property of time invariance of R, T, R' and T'. The result is only obtained in the continuous mode [27,28] in which all the generated waves interfere to destroy the initial reflected wave.

In time-reversal mirrors, such effects cannot be used. We work with pulsed waves in the transient regime. On the one hand, the impulse waves generated along the interface cannot interfere. On the other, *the recording step does not overlap with the transmitted step* and the different time-reversed waves cannot interfere with the incident waves. Therefore, a single TRM located in medium 2 can neither cancel the wave of amplitude R reflected on the 1 to 2 interface, nor generate a time-reversed wave of amplitude 1 in medium 1. In order

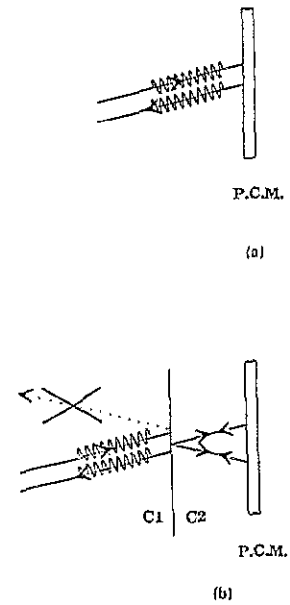

Figure 15. (*a*) Principle of the PCM. An incident monochromatic plane wave is reflected and phase-conjugated. The wavevector of the phase-conjugated wave is reversed relative to the incident wavevector. (*b*) The effect of PCM on phase velocity discontinuities. An incident plane wave induces along the interface the generation of a complicated set of waves. Owing to the multiple reflections between the interface and the PCM, the resulting field in medium 1 reduces to the phase-conjugation of the incident wave. There is complete destructive interference in the direction of the initial reflected wave.

to obtain this time-reversed wave, a second TRM has to be placed in medium 1 behind the incident wave source [23]. This set of two TRMs is equivalent to a TR cavity.

4.3. Ultrasonic phase-conjugated mirrors

Although our time-reversal approach developed for an ultrasonic field is quite different from the phase-conjugation approach, different authors have developed ultrasonic phase-conjugated mirrors based on the use of monochromatic signals and nonlinear effects [29].

The basic method used to produce phase-conjugated wavefronts is to mix the incident wavefront in space with a wavefield oscillating with a frequency twice that of the incident radiation. This approach requires an elastically nonlinear medium within which mixing can be carried out. Piezoelectric or ferromagnetic media can be used to process the nonlinear mixing. Ohno [30] has studied such an effect with a $LiNbO_3$ piezoelectric crystal working at 50 MHz. The incident wavefront propagating in the crystal is mixed with an electric field oscillating on the second harmonic. Brysev [31] has developed such a parametric interaction in a Ni-ferrite polycrystal by mixing the incident wavefront with an oscillating magnetic field that modulates the sound velocity in the ferrite. Sato [32,33] has used suspended microparticles as the nonlinear medium.

Another original technique has been developed by Nikoonahad [34]. The PCM is based, as in the TRM approach, on a transducer array that samples an incident monochromatic wavefront. The signals collected from

each array element are electronically mixed with a second-harmonic signal, using an array of mixers. The difference frequency signal so obtained has a phase that is the conjugate of that of the incident wavefront. The transducer array then retransmits the conjugated signals. One limitation of the technique is the continuous wave mode operation. Also, in principle, the phase-reversed signals have to be fed back to the same array element at which the wavefront was sampled and this results in a short-circuit across the two ports of the mixer. To overcome this difficulty, Nikoonahad feeds the conjugated signals to the element immediately adjacent to where the wavefront was sampled. The transducer array is then made of two sets of interlaced elements: those that sample the wavefront and those that transmit the conjugated wavefront. In order to avoid phase shift due the spatial offset, the array pitch has to be $\lambda/4$.

5. The iterative time-reversal mode

5.1. Automatic target selection

One major advantage of the TRM is the ability to choose the origin and duration of the signals to be time-reversed. This is done by definition of the temporal window that selects the data to be time-reversed. When the medium of interest contains several reflectors, the time-reversal technique cannot directly be focused on one point. Indeed, if the medium contains two targets of different reflectivity illuminated by a short pulse, time-reversal of the echoes reflected from these targets will generate two wavefronts refocused on each target. The mirror produces the real acoustic images of the two reflectors on themselves. The highest amplitude wavefront illuminates the most reflective target, while the weakest wavefront illuminates the second target. However, what we have described is, in fact, only valid if we neglect the multiple-scattering processes which can occur between the two targets. In order to avoid these multiply scattered waves, we can select echoes within a particular time-reversal window. In this case, the time-reversal process can be iterated [1, 2, 22]. After the first time-reversed illumination, the weakest target will be illuminated more weakly and will reflect a wavefront much fainter than the one coming from the strongest target (figure 16). After some iterations, the process will converge and produce a wavefront focused on the most reflective target. This process converges if the target separation is sufficient to avoid illumination of one target by the real acoustic image of the other target [22, 23]. In the case of a multi-target medium the convergence problem is more complicated and has been studied with great care by Prada [35].

Although this simple presentation implies the iterative mode is very attractive, one can argue that a contradiction exists between the concept of iteration and the physical principle of time-reversal invariance. Indeed, the complete time-reversal of an acoustic 'scene'

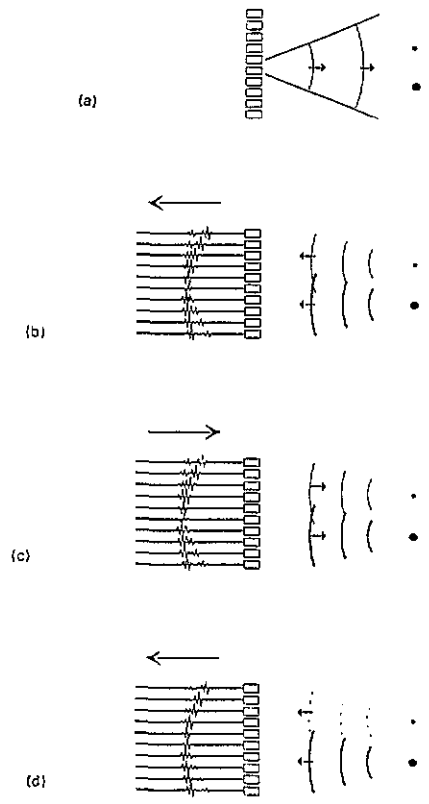

Figure 16. Principle of the iterative time-reversal mode. (*a*) A first transmitted wave illuminates a sector containing the two targets. (*b*) The reflected waves are recorded on the array. (*c*) The data are time-reversed and re-emitted. The time-reversed wavefronts refocus on the two targets. The highest amplitude wavefront illuminates the most reflective target, while the weakest wavefront illuminates the second target. (*d*) The new reflected wavefronts are recorded before another time-reversal. Note that the weakest target has been illuminated more weakly and reflects a wavefront much fainter than the one coming from the strongest target. After some iterations the process will converge and produce a wavefront focused on the most reflective target.

results in the time-reversed scene. Therefore, iteration of the time-reversal operation gives stationary results, in contradiction with wavefield modification after each iteration. In fact, the contradiction is only apparent. A complete time-reversal operation requires a closed time-reversal cavity surrounding the acoustic scene and a recording time T long enough to take into account all the multiply scattered waves. In our technique, we utilize only a finite spatial aperture and short temporal windows. Therefore, some information is lost. This information loss gives the iterative mode its target-selection capabilities.

Experiments have been performed with TRM2 to demonstrate the ability of the TRM iterative mode to select the most reflective target in a multi-target medium. The medium is made of two different wires situated at a depth $z = 110$ mm from the array. The two wires are parallel to the long axis of each array element (figure 17) and they are located on each side of the array axis. A 1.5 mm diameter copper wire is located 7 mm away from the array axis and a 0.7 mm brass wire is located 13 mm from the axis.

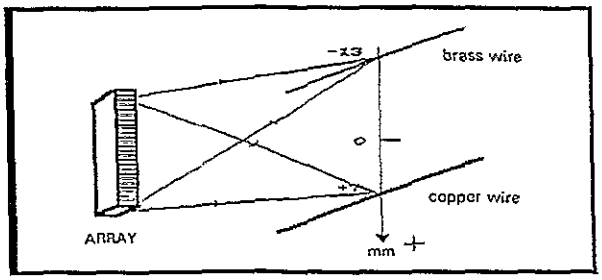

Figure 17. Configuration of the multi-target experiment. Two different wires are located at a depth $z = 110$ mm from the plane linear array TRM2.

In the first step TRM2 illuminated an angular sector containing the two wires. The illuminated beam was transmitted by a single transducer element located at the array centre. The directivity pattern of a single element is wide. After the first illumination, the echoes from the two targets were recorded. Figure 18(*a*) shows the recorded data corresponding to two individual wavefronts pointing at the two wires. The recorded signals were then time-reversed and retransmitted. The time-reversed waves propagated and the new directivity pattern was measured by scanning the plane $z = 110$ mm with the hydrophone. Figure 18(*b*) represents the directivity pattern which clearly shows two maxima corresponding to the two target locations. The pressure field reaches a higher value at the location of the copper wire, whose scattering cross section is larger than that of the brass wire. The process was iterated: the new echoes from the wires were recorded, time-reversed and retransmitted, and so on. As the process was iterated, the brass wire which reflects less energy received a weaker time-reversed wave. This is clearly shown in figures 18(*b*), (*d*) and (*h*) which correspond to the directivity pattern of the first, second and third iterations. The brass wire is no longer illuminated after the last illumination. Figures 18(*c*), (*e*) and (*g*) represent the reflected wavefronts recorded by the array after the first, second and third iterations. At the end of the iteration process (figure 18(*g*)) only the echoes from the most reflective target remain.

Two particular points may be emphasized.

(i) Figures 18(*a*), (*c*), (*e*) and (*g*) show that the echo duration becomes longer after each iteration. This is due to multiple convolution of the pressure signals by the acoustoelectric impulse response of the transducer elements.

(ii) The echo pattern shown in figure 18(*a*) is more complex than the simple description given previously. In fact, the two wavefronts are followed by weaker replicas. These replicas correspond to surface waves propagating around the wires generated by mode conversion of the incident wave into surface waves. The wires cannot be assumed to be point-like targets. They behave as extended sources.

When the process is iterated, target resonances can intensify by the time-reversal procedure and figure 18(*g*) shows two replicas appearing symmetrically before and after the principal wavefront. The wire diameter can be estimated by measurement of the time shift between the replica and the principal wave.

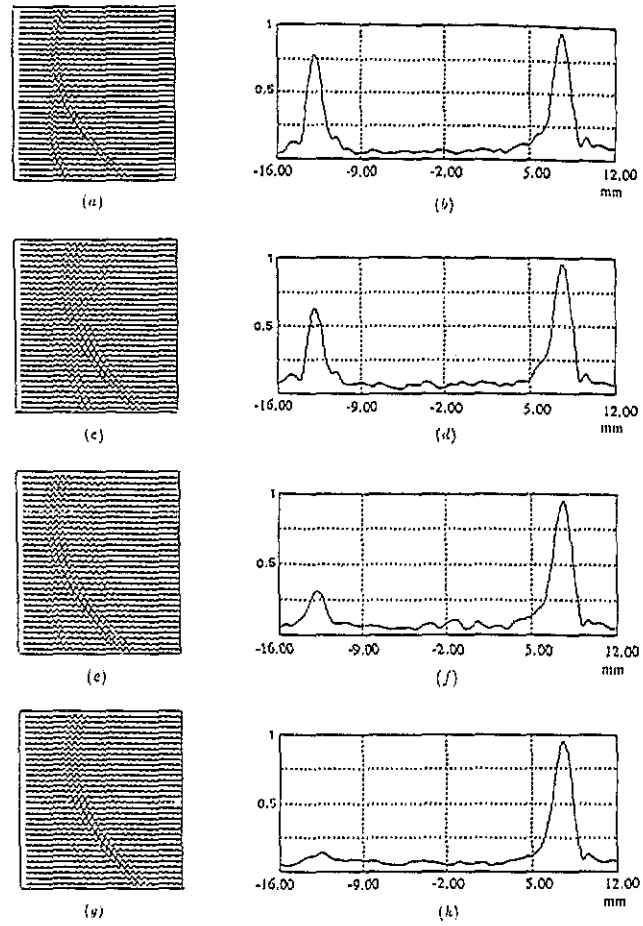

Figure 18. Selective focusing in the case of two wires. The time-reversal process is iterated. (*a*), (*c*), (*e*) and (*g*) show the echographic signals recorded from the two wires after the first illumination (*a*) and the first (*c*), second (*e*) and third (*g*) iteration of the time-reversal process. (*b*), (*d*), (*f*) and (*h*) represent the pressure diagrams observed in the wire plane after the first time-reversal process (*b*) and its iterations.

These experiments demonstrate the ability of the TRM iterative mode to select the most reflective target in a multi-target medium. This may be viewed as a learning process that selects from among several wavefronts the one coming from the most important reflector. However, with extended targets, the process is complicated by target resonances.

5.2. Extended targets and the inverse problem

In echographic applications that deal with extended targets, the time-reversal process is complicated by the fact that a target is not point-like. An incident beam induces two kinds of reflected waves: a first reflected wavefront, which is only related to the target geometry, and a second set of multiply reflected wavefronts generated by mode conversions of the incident wave into surface waves and volume waves propagating around or inside the target (figure 19(*a*)). The first reflected wavefront results from the interference pattern of the

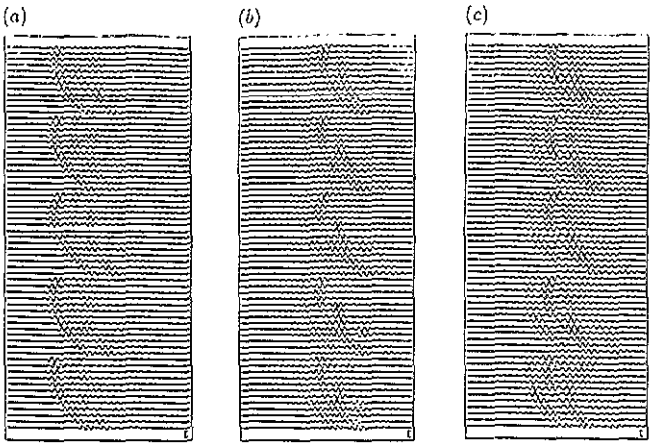

Figure 19. Echographic signals recorded on the five transducer rows from the kidney stone: (*a*) for illumination by a single transducer element; (*b*) after the first iteration; and (*c*) after the second iteration.

wavelets scattered by each elementary surface element. Taking into account the directivity pattern of each scattered wavelet, which depends on the angle between the incident beam axis and the normal vector to the elementary surface, the target can be considered as a continuous set of point-like targets of different scattering strengths. The second set of reflected waves is directly related to acoustical resonances of the target. The different surface waves are generated on the extended target at particular locations where the mode conversions occur. In the same way, the surface waves turn around the target and are continuously mode-converted and generate in the fluid a set of reflected waves. Time-reversal of these particular waves may be used to produce strong target resonances. On the other hand, time-reversal of the first reflected wavefront will generate a wavefront matched to the target surface. The mirror, processing only the first reflected wavefront, produces the real acoustic image of the extended target on itself. After some iterations of the 'first reflected wavefront time reversal' the process will converge and produce a wavefront focused on the most reflective spot of the target. When the time-reversal process deals with the complete set of reflected waves, the process is complicated by the target resonances and will converge on a spot which is not always the most reflective spot, but can be related to the locations where the surface waves are mode converted into reflected waves. Such a process is quite complicated and has been studied in our laboratory by Thomas and Roux for targets of well-defined geometry such as cylindrical and spherical reflectors of dimensions greater than the wavelength [36]. Time-reversal techniques appear to be a new way to solve the inverse problem in ultrasonic scattering.

5.3. Lithotripsy experiments

In lithotripsy experiments kidney stones are extended targets. The mirror we use is a two-dimensional prefocused mirror working at 1 MHz (TRM4) [24]. It is part of a two-dimensional curved array. Each transducer element is a plane disc of 6 mm diameter and the 64

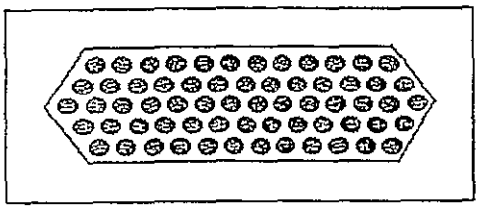

Figure 20. Geometry of the prefocused two-dimensional mirror. The disc plane transducers are distributed according to a structure of five rows of respectively 12, 13, 14, 13 and 12 elements.

elements are arranged on a spherical cup of 120 mm radius of curvature. The transducers are in a hexagonal mesh and distributed according to a five-row structure of respectively 12, 13, 14, 13 and 12 elements (figure 20). The maximum aperture of the array is 120 mm.

The first experiment was performed with one kidney stone placed 100 mm from the surface of the mirror. The shape of the kidney stone was irregular. Its largest dimension was about 10 mm. The kidney stone was located between 10 and 20 mm away from the mirror central axis.

In the first step, TRM4 illuminated an angular sector containing the kidney stone. The illuminating beam was transmitted by a single transducer element located at the centre of the array. After the first illumination, the echoes from the stone were recorded. Figure 19(*a*) presents the recorded data. We notice that the signals correspond to the five transducer rows used in TRM4. They line up along five wavefront sections. Figure 20(*a*) shows clearly the first reflected wavefront and the successive wavefronts generated by surface wave conversion. Depending on the transducer element, one or two replicas of the primary wavefront can be observed.

In the second step of the experiment, the recorded signals shown in figure 19(*a*) are time-reversed and retransmitted. The time-reversed waves propagate and the pressure pattern is measured in the kidney stone plane with the hydrophone (the kidney stone frame has been removed). Figure 21(*a*) shows the directivity pattern along an axis parallel to the transducer rows and passing through the TRM4 central axis. The diagram is plotted between 10 and 20 mm off axis, corresponding to the previous stone location. It can be noticed that this diagram does not vanish at the stone boundaries. This is explained by the fact that the stone is an asymmetrical target and that TRM4 is only part of a full two-dimensional mirror (14 transducers along one direction and 5 along the orthogonal direction). Some information about the stone shape is lost and the time-reversal process is not completely effective. The stone has several sides acting as specular reflectors oriented only in some particular directions, and some part of the reflected beams is not recorded by the limited aperture of TRM4. The stone reconstruction (the real acoustic image) requires interference of all the time-reversed beams and a null pressure field outside the stone location also requires complete destructive interference.

To overcome this difficulty, the time-reversal process can be iterated. After the first time-reversed

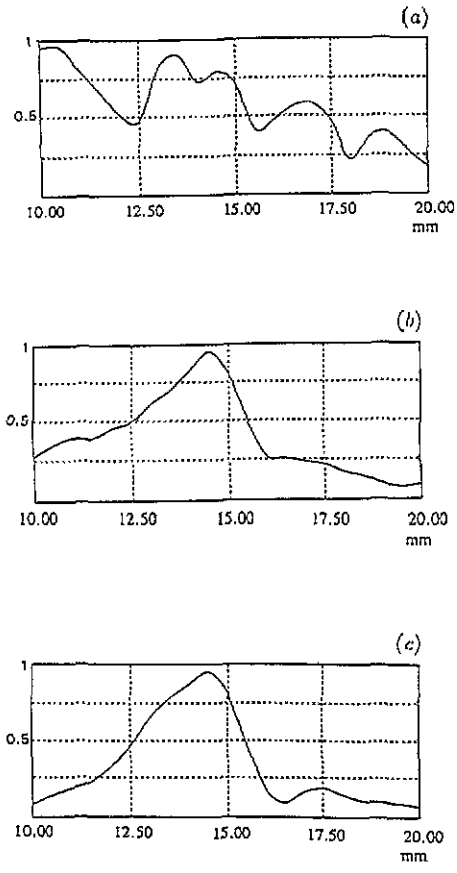

Figure 21. TRM focusing on a kidney stone. Directivity patterns in the kidney stone plane are shown in (a) for the first time-reversal illumination. The pressure pattern is shown in (*b*) and (*c*) for the first and second iterations respectively.

transmission, the new echoes from the stone can be recorded, time-reversed and retransmitted and so on. Figures 21(*b*) and (*c*) represent the new pressure pattern after the first and the second iterations, while figures 19(*b*) and (*c*) represent the echoes from the stone after the first and second iterations. Figures 21(*b*) and (*c*) show that after the first iteration the time-reversal process selects a small spot on the extended target and focuses on it. In the second iteration, the TRM transmits a relatively narrow beam that intercepts the kidney stone. The −6 dB beamwidth is equal to 4.2 mm whereas the kidney stone width is at least 10 mm. We have conducted TRM experiments on many kidney stones and have observed the same converging process in all the cases. After one or two iterations, the TRM selects a small portion of the extended target and the resulting beam focuses on a spot whose dimension is of the order of the diffraction point spread function.

In another experiment, we increased the complexity to simulate real situations. The experimental geometry was seriously complicated by the introduction of two kidney stones of similar dimensions behind a strong aberrator (figure 22). The aberrating medium was again made of a thick silicone layer whose thickness is randomly modulated with a maximum thickness of 15 mm and a standard deviation of about 3 mm. The coherence length of the aberrator at 1 MHz is about

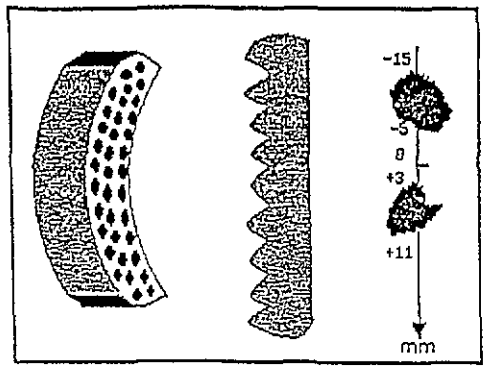

Figure 22. Geometry of the kidney stones experiment. The two kidney stones are located in the plane $z = 110$ mm, the aberrator is placed between the stones and the prefocused two-dimensional array.

15 mm. The aberrator front side was located at a depth $z = 60$ mm from the array surface. The two kidney stones were located at a depth $z = 110$ mm. The smaller kidney stone was located between +3 mm and +11 mm from the axis and the largest one between −5 mm and −15 mm (figure 22).

In the first step, the central element of the array illuminated an angular sector that contained the stones. The echoes from the stones were recorded, time-reversed and re-emitted. Figure 23(*a*) shows the time-reversed pressure pattern in the plane $z = 110$ mm. Similarly to the previous section, we observe that the first time-reversed beam does not focus on the two stones. After the first iteration of the time-reversal process, a pressure peak appears clearly at −9 mm from the axis (figure 23(*b*)). It corresponds to a point located on one of the kidney stones (the one located on the negative side of the array axis). A smaller peak also appears at +7 mm, corresponding to the other kidney stone. After two more iterations, the peak corresponding to the second kidney stone (on the positive side) disappears (figures 23(*c*) and (*d*)). Only one peak remains (at −9 mm from the axis), but with significant secondary lobes. The lobe level can be reduced using a larger TRM aperture. This experiment shows that, even in a complicated case, the time-reversal mirror is able to select one stone and focus on a small portion of it, even through a strongly aberrating medium.

Since these experiments were conducted, a new fully parallel real-time electronic prototype has been built allowing a complete time-reversal operation in 1 ms. This prototype is now being used, with complete two-dimensional prefocused mirrors working in a lower frequency range (400 kHz), for *in vivo* experimentation on gall bladder and kidney stones.

6. Conclusion

Time-reversal of ultrasonic fields is a new tool in applied physics. Time-reversal mirrors are made of large transducer arrays connected to large storage memories. They make possible a very efficient way to focus an ultrasonic wave through inhomogeneous media. Their applications are numerous and concern medical

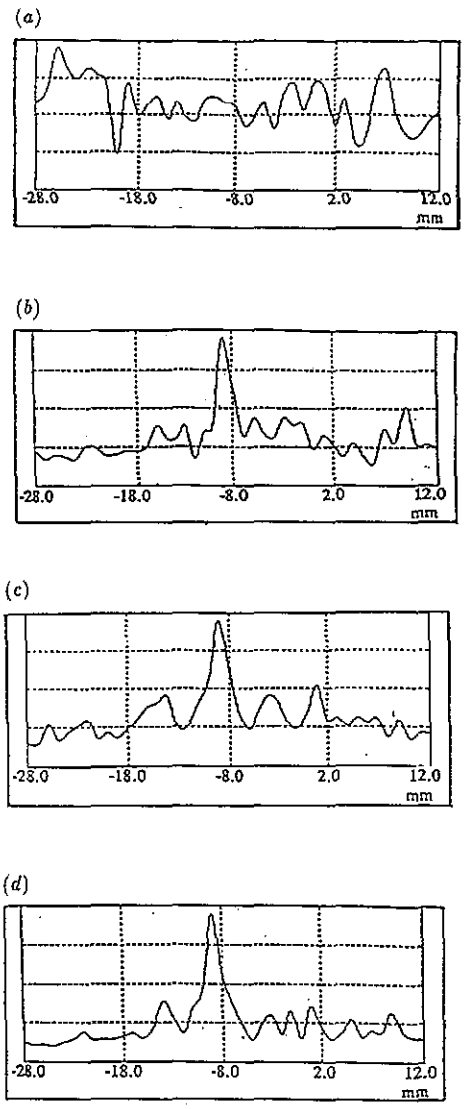

Figure 23. Directivity patterns in the plane $z = 110$ mm: (*a*) for the first time reversal illumination; (*b*), (*c*) and (*d*) for the first, second and third iterations.

applications (imaging, lithotripsy and hyperthermia) as well as non-destructive testing and underwater acoustics.

Experimental results obtained with 64 and 128 channel time-reversal mirrors demonstrate the possibilities of this technique and several companies are now working on the development of ultrasonic time-reversal mirrors. However, time-reversal mirrors are not only devoted to applied physics. They can also be used in fundamental physics to solve some problems in the field of wave propagation. Inverse problems can be solved by use of a TRM and preliminary studies are being published [36]. The TRMs can also be used to study multiple-scattering processes in heterogeneous media and to give some new approaches to the problem of wave localization.

References

[1] Fink M, Prada C, Wu F and Cassereau D 1989 Self focusing with time reversal mirror in inhomogeneous media *Proc. IEEE Ultrasonics Symp. 1989, Montréal* vol 2, pp 681–6

[2] Fink M 1992 Time reversal of ultrasonic fields: basic principles *IEEE Trans. Ultrason. Ferroelectr. Freq. Control* **39** 555–66

[3] Muller R A and Buffington A 1974 Real-time correction of atmospherically degraded telescope images through image sharpening *J. Opt. Soc. Am.* 1200–10

[4] Buffington A, Crawford F S, Muller R A, Schwemin A J and Smits R G 1977 Correction of atmospheric distortion with an image sharpening telescope *J. Opt. Soc. Am.* 298–303

[5] Pepper D M 1988 Non linear optical phase conjugation *Laser Handbook* vol 4 (Amsterdam: North-Holland) pp 333–485

[6] Flax S W and O'Donnel M 1988 Phase aberration correction using signals from point reflectors and diffuse scatterers: basic principles *IEEE Trans. Ultrason. Ferroelectr. Freq. Control* **35** 758–67

[7] O'Donnel M and Flax S W 1988 Phase aberration correction using signals from point reflectors and diffuse scatterers: measurements *IEEE Trans. Ultrason. Ferroelectr. Freq. Control* **35** 768–74

[8] Nock L, Trahey G E and Smith S W 1989 Phase aberration correction in medical ultrasound using speckle brightness as a quality factor *J. Acoust. Soc. Am.* **85** 1819–33

[9] Trahey G E, Zhao D, Miglin J A and Smith S W 1990 Experimental results with a real-time adaptive ultrasonic imaging system for viewing through distorting media *IEEE Trans. Ultrason. Ferroelectr. Freq. Control* **37** 418–29

[10] Mallart R and Fink M 1992 Sound speed fluctuations in medical ultrasound imaging. Comparison between different correction algorithms *Proc. 19th Int. Symp. Acoustical Imaging* (New York: Plenum) pp 213–19

[11] Mallart R and Fink M 1991 The Van Cittert–Zernike theorem in pulse-echo measurements *J. Acoust. Soc. Am.* **90** 2718–27

[12] Wu F, Fink M, Mallart R, Thomas J L, Chakroun N, Cassereau D and Prada C 1992 Optimal focusing through aberrating media: a comparison between time reversal mirror and time delay correction techniques *Proc. IEEE Ultrasonics Symp. 1991, Orlando* pp 1195–1201

[13] Morse P M and Ingard K U 1968 *Theoretical Acoustics* (New York: McGraw-Hill)

[14] Hecht E 1987 *Optics* (New York: Addison-Wesley) pp 118–20

[15] Nieto-Vesperinas M and Wolf E 1985 Phase conjugation and symmetries with wave fields in free space containing evanescent components *J. Opt. Soc. Am.* **2** 1429–34

[16] Porter R P and Devaney A J 1982 Generalized holography and the inverse source problems *J. Opt. Soc. Am.* **72** 327–30

[17] Cassereau D, Wu F and Fink M 1991 Limits of self-focusing using closed time-reversal cavities and mirrors–theory and experiment *Proc. IEEE Ultrasonics Symp. 1990 Hawaii* pp 1613–8

[18] Cassereau D and Fink M 1992 Time-reversal of ultrasonic fields: theory of the closed time-reversal cavity *IEEE Trans. Ultrason. Ferroelectr. Freq. Control* **39** 579–92

[19] Kino G S 1987 *Acoustics Waves* (New York: Prentice Hall)

[20] Agarwal G S, Friberg A T and Wolf E 1982 Elimination of distortions by phase conjugation without losses or gains *Opt. Commun.* **43** 446–50

[21] Agarwal G S and Wolf E 1982 Theory of phase conjugation with weak scatterers *J. Opt. Soc. Am.* **72** 321–6

[22] Prada C, Wu F and Fink M 1991 The iterative time reversal mirror: a solution to self focusing in pulse-echo mode *J. Acoust. Soc. Am.* **90** 1119–29

[23] Prada C 1991 *Retournement temporel des ondes ultrasonores* Thèse de Doctorat de l'Université de Paris VII

[24] Wu F, Thomas J L and Fink M 1992 Time reversal of ultrasonic fields: experimental results *IEEE Trans. Ultrason. Ferroelectr. Freq. Control* **39** 567–78
[25] Chakroun N, Fink M and Wu F Ultrasonic non destructive testing with time reversal mirrors *Proc. IEEE Ultrasonics Symp. 1992, Tucson*
[26] Mittra R and Habashy T M 1984 Theory of wave-front distortion correction by phase conjugation *J. Opt. Soc. Am.* **1** 1103–9
[27] Friberg A T and Drummond P D 1983 Reflection of a linearly polarized plane wave from a lossless stratified mirror in the presence of a phase conjugate mirror *J. Opt. Soc. Am.* **73** 1216–9
[28] Lindsay I Specular reflection cancellation/enhancement in the presence of a phase conjugate mirror *J. Opt. Soc. Am.* B **4** 1809–15
[29] Bunkin F V, Kravtsov Yu A and Lyakhov G A 1986 Acoustic analogues of non linear optics phenomena *Sov. Phys.–Usp* **29** 607–19
[30] Ohno M 1989 Generation of acoustic phase conjugate waves using nonlinear electroacoustic interaction in $LiNbO_3$ *Appl. Phys. Lett.* **54** 1979–80
[31] Brysev A P, Bunkin F V, Ekonomov N A and Krutiansky L M 1990 Giant regenerative amplification with sound wave phase conjugation in ferrite *Proc. Premier congrès Français d'acoustique, Lyon, J. Physique Suppl.* **2** 73–6
[32] Sato T, Nakayama T, Yamashoki Y and Katakoa Y 1988 Ultrasonic phase conjugator using a microparticle suspended cell and novelty imaging *Ultrason. Imaging* **10** 68
[33] Sato T, Kataoka H, Nakayama T and Yamakoshi Y 1988 Ultrasonic phase conjugator using micro particle suspended liquid cell *J. Acoust. Soc. Japan* **44** 122–9
[34] Nikoonahad M and Pusateri T L 1989 Ultrasonic phase conjugation *J. Appl. Phys.* **66** 4512–3
[35] Prada C, Thomas J L and Fink M 1993 The iterative time reversal process: analysis of the convergence *J. Acoust. Soc. Am.* submitted
[36] Thomas J L, Roux P and Fink M 1993 Inverse problem in wave scattering with an acoustic time reversal mirror *Phys. Rev. Lett.* submitted